Trung Duc Pham, 2026, 14:4
ISSN (Online): 2348-4098
ISSN (Print): 2395-4752

International Journal of Science, Engineering and Technology
An Open Access Journal

Crosswind Effects on the Aerodynamic Characteristics of the L-39NG During the Flare Phase of Landing Using ANSYS CFX

[1]Trung Duc Pham
[1]Air Force Officer's College, Khanh Hoa, Vietnam

Abstract- In aviation operations, the landing phase, particularly the flare stage, plays a critical role, directly affecting flight training quality and flight safety. This paper investigates the influence of crosswind on the aerodynamic characteristics of the L-39NG aircraft using numerical simulation with Ansys software. The results show that crosswind increases drag, reduces lift, and generates lateral force, thereby affecting stability and controllability during landing. The study provides a scientific basis for improving operational efficiency and enhancing aircraft safety.

Keywords— L-39NG; Flare phase; Crosswind; Aerodynamic characteristics

I. INTRODUCTION

Landing is one of the most critical and complex phases of flight, during which the aerodynamic behavior of an aircraft is significantly influenced by environmental conditions, particularly crosswind. For the L-39NG, crosswind induces a sideslip angle β, disrupts the symmetry of the surrounding airflow, and consequently alters lift, drag, side force, and aerodynamic moments, directly affecting aircraft stability and controllability during the flare phase.

To quantify these aerodynamic changes, computational fluid dynamics (CFD) simulations were performed using ANSYS to resolve the flow field and determine the aerodynamic coefficients under different crosswind conditions.

This approach enables detailed visualization of the airflow around the model and numerical evaluation of aerodynamic forces and moments under conditions that are difficult to investigate analytically or experimentally. In this study, the L-39NG in landing configuration was analyzed at several sideslip angles to clarify the influence of crosswind on aerodynamic characteristics during the flare phase, thereby providing a technical basis for assessing operating conditions and landing safety.

II. METHODOLOGY

1. Geometric Modeling and Meshing

A full-scale three-dimensional geometric model of the L-39NG aircraft was developed in ANSYS based on geometric data from technical documentation and direct measurements. The fuselage was generated from a series of elliptical sections varying along the longitudinal direction; the main wing uses the NACA 2508 airfoil, whereas the horizontal and vertical tails use the NACA 0008 airfoil.

To represent the landing configuration during the flare phase, the model was configured with the landing gear extended, flaps deflected to 44°, the speed brake retracted, and the rudder and ailerons in their neutral positions.

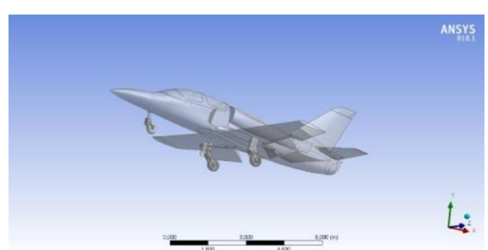

Figure 1: Three-dimensional geometric model of the L-39NG aircraft.

The computational domain was constructed around the entire aircraft with sufficiently large dimensions

© 2026 Trung Duc Pham This is an Open Access article distributed under the terms of the Creative Commons Attribution License (http://creativecommons.org/licenses/by/4.0), which permits unrestricted use, distribution, and reproduction in any medium, provided the original work is properly credited.

to minimize the influence of the outer boundaries on the near-field flow. The domain dimensions were selected within the ranges ($10b_0$-$15b_0$) × ($6b_0$-$8b_0$) × ($6b_0$-$10b_0$), where b_0 is the wing root chord.

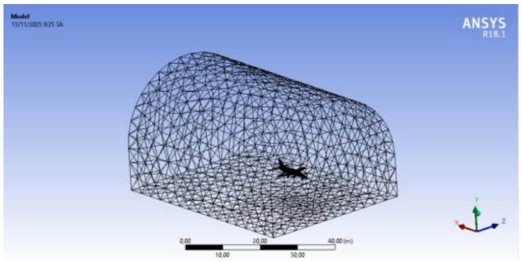

Figure 2: Computational domain for the L-39NG aerodynamic simulation

The upper portion of the computational domain was configured with a semicircular cross-section to reduce unnecessary domain volume and computational cell count. The aircraft was positioned at an altitude of H = 9 m, corresponding to the flare phase. The computational mesh was generated using ANSYS Meshing, with local refinement near the aircraft surface and progressively coarser elements toward the outer boundaries. This strategy improves the resolution of near-body flow gradients while reducing computational cost. The mesh was adjusted to ensure a smooth transition in element size and to limit mesh distortion, thereby improving convergence behavior and the reliability of the numerical solution.

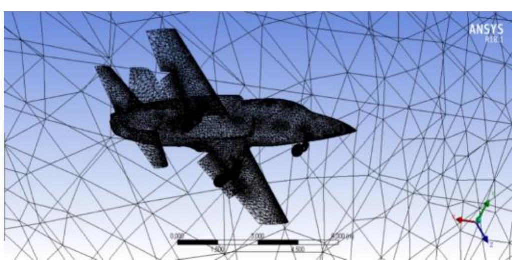

Figure 3: Computational mesh of the flow domain and mesh refinement around the L-39NG aircraft

Inputting Boundary Parameters and Problem Setup

After meshing, the fluid properties and boundary conditions were defined in ANSYS CFX. The airflow was assumed to be steady, subsonic, and viscous, with an ambient pressure of P = 101325 Pa, air density ρ = 1.225 kg/m^3, and kinematic viscosity ν = 1.553×10^{-5} m^2/s. The k-ε turbulence model was employed throughout the simulations.

The aircraft surface was defined as an impermeable adiabatic wall. At the inlet, a subsonic flow condition with a turbulence intensity of 5% was prescribed, while the outlet and outer boundaries were specified in accordance with external-flow conditions. The simulations were conducted at an altitude of H = 9 m and a flight speed of V = 55.56 m/s, with the angle of attack α varied from 0° to 16°. Crosswind effects were represented by sideslip angles β = 5°, 11°, and 15°, corresponding to progressively increasing crosswind levels; the β = 0° case was used as the no-crosswind baseline.

The convergence criterion was set to 10^{-4}, with a maximum of 100 iterations. All simulation cases were computed using the same numerical and boundary-condition settings to ensure consistent comparison of the aerodynamic characteristics as functions of angle of attack and sideslip angle.

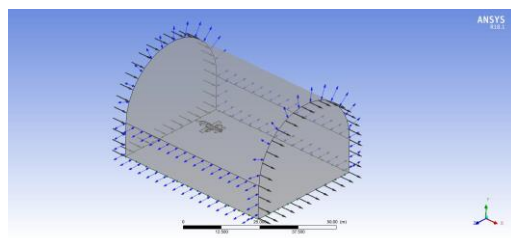

(a)

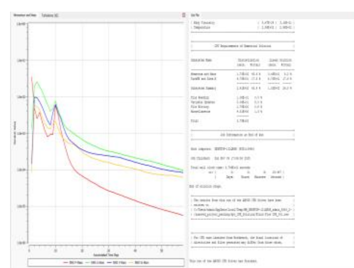

(b)

Figure 4: Boundary-condition setup and convergence history of the L-39NG numerical simulation:

(a) Boundary-condition setup; (b) convergence history

Model Validation

The numerical model was evaluated for the no-crosswind condition at V=55.56m/s, α=6o, and β=0o. ANSYS CFX predicted a lift coefficient of Cy=1.18, while the theoretical value calculated from the lift–weight equilibrium condition was Cy=1.108. The relative difference was approximately 6.50%, indicating reasonable agreement and supporting the use of the numerical model for the subsequent crosswind simulations.

III. RESULTS AND DISCUSSION

Visual Representation of the Flow Field Around the Model

To visualize the influence of crosswind on the flow around the L-39NG, the velocity field and pressure distribution were examined at a representative angle of attack of α = 10° for four conditions: no crosswind (β = 0°), light crosswind (β = 5°), near-limit crosswind (β = 11°), and strong crosswind (β = 15°). The results were compared using two characteristic viewing directions along the X- and Y-axes.

Viewed along the X-axis, the flow field in the no-crosswind case (β = 0°) is essentially symmetric about the aircraft longitudinal plane. As crosswind is introduced, this symmetry is progressively disrupted. At β = 5°, the flow deflection remains relatively small; at β = 11°, the airflow is displaced more clearly to one side and a noticeable pressure difference develops between the windward and leeward sides. At β = 15°, the asymmetry and flow disturbance become most pronounced.

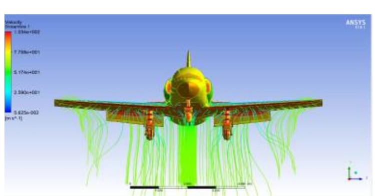

(a)

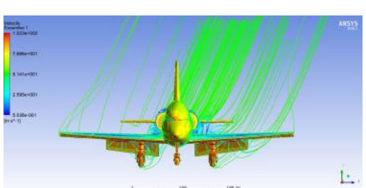

(b)

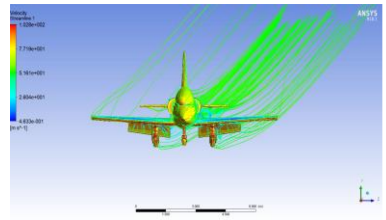

(c)

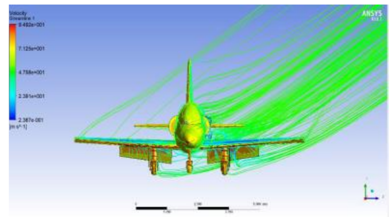

(d)

Figure 5: Flow-field and pressure distribution around the L-39NG aircraft viewed along the x-axis at different

Sideslip Angles

(a) β=0o, (b) β=5o, (c) β=11o, and (d) β=15o

The view along the Y-axis provides a clearer indication of the airflow changes along the fuselage and wings. At β = 5°, the flow is already asymmetric, although the degree of distortion remains limited. As β increases to 11° and 15°, the streamlines are strongly deflected in the crosswind direction, and the bilateral symmetry of the flow around the aircraft is clearly destroyed.

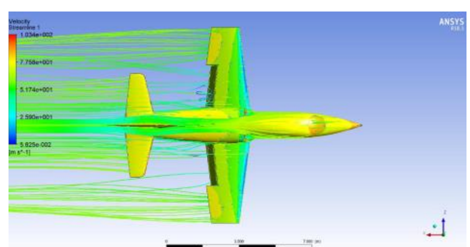

(a)

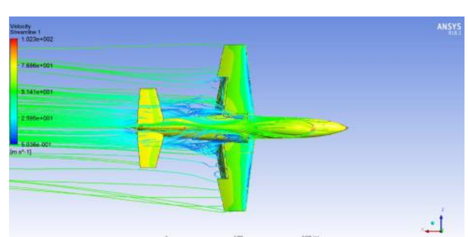

(b)

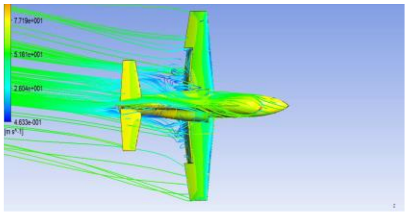

(c)

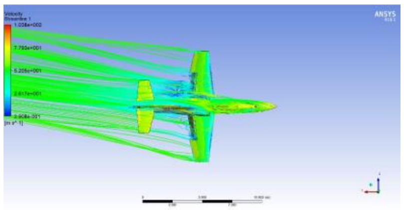

(d)

Figure 6: Flow-field and pressure distribution around the L-39NG aircraft viewed along the y-axis at different

Sideslip Angles

(a) β=0o, (b) β=5o, (c) β=11o, and (d) β=15o

Overall, as the sideslip angle increases from 0° to 15°, the flow field around the aircraft evolves from a nearly symmetric state to a strongly asymmetric one. This change demonstrates that crosswind significantly modifies the flow structure around the fuselage and wings, providing a physical basis for the variations in aerodynamic force and moment coefficients discussed in the following section.

Evaluation of Lift and Drag Characteristics Extracted from the Software

Based on the ANSYS CFX results, the drag coefficient Cx and lift coefficient Cy of the L-39NG were determined over an angle-of-attack range of α = 0°-16° for four sideslip conditions, β = 0°, 5°, 11°, and 15°. In the no-crosswind case, the lift coefficient increases with angle of attack and reaches Cymax = 1.698 at α = 16°. When the angle of attack is further increased to 17.5° and 20°, Cy decreases to 1.607 and 1.345, respectively, indicating the onset of flow separation and stall. Therefore, the crosswind analysis was restricted to α ≤ 16°.

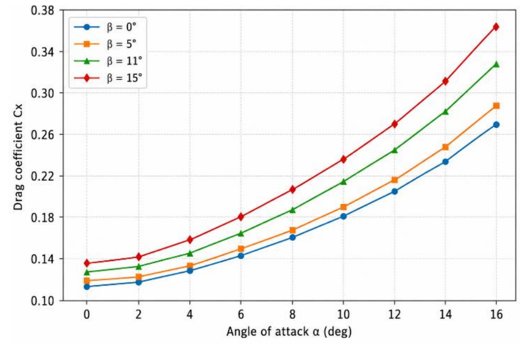

Figure 7: Variation of drag coefficient Cx with angle of attack at different sideslip angles

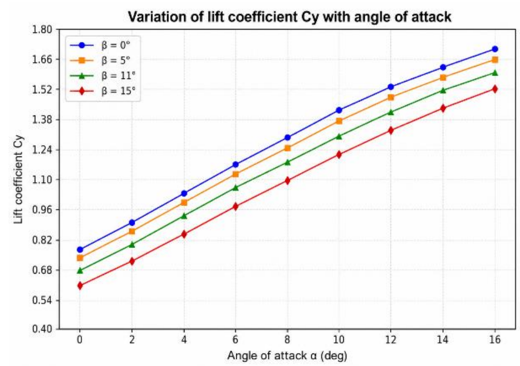

Figure 8: Variation of lift coefficient Cy with angle of attack at different sideslip angles

The plots show that under light-crosswind conditions (β = 5°), the aerodynamic-characteristic curves begin to deviate from the baseline case (β = 0°), although the overall difference remains relatively small. Both the drag coefficient Cx and the lift coefficient Cy exhibit only slight variations.

Under the near-limit crosswind condition (β = 11°), the Cx curve rises considerably more steeply than for β = 5°, particularly at high angles of attack, with the increase in drag exceeding 21%. At the same time, the Cy curve shifts downward, indicating that the aircraft generates less lift at the same angle of attack as the sideslip angle increases.

Under the strong crosswind condition, beyond the allowable crosswind level (β = 15°), the aerodynamic curves exhibit the largest deviation from the other cases, demonstrating severe degradation of aerodynamic performance. The Cx curve increases sharply; at α = 16°, the drag coefficient is more than 35% higher than in the no-crosswind case. This increase is associated with the large sideslip condition, which raises the aerodynamic drag contribution and causes pronounced distortion of the flow field around the aircraft.

IV. CONCLUSION

Using numerical simulations in ANSYS CFX, this study evaluated the influence of crosswind on the aerodynamic characteristics of the L-39NG during the landing flare. The results show that the magnitude of the aerodynamic effects increases markedly with increasing sideslip angle β. The principal conclusions are as follows:

- For light crosswind (β = 5°): The aircraft remains capable of a safe landing using standard control techniques. Attention should be paid to the slight increase in drag and the appearance of side force, with appropriate corrective control inputs applied as required. The available lift margin remains sufficient for safe landing.
- For crosswind near the allowable limit (β = 11°): This condition is close to the operational crosswind limit. The aerodynamic characteristics deteriorate significantly, with the aerodynamic efficiency K decreasing by more than 19%. Landing under this condition requires greater pilot experience, careful management of approach speed to compensate for the reduction in lift, and readiness to execute a go-around if the crosswind does not decrease.
- For hazardous crosswind (β = 15°): The aerodynamic characteristics deteriorate severely, with the drag coefficient increasing by more than 17.95%, the lift coefficient decreasing by more than 10%, and the aerodynamic efficiency decreasing by more than 32%. The aerodynamic moments reach adverse levels, resulting in a highly demanding control condition. According to the applicable technical limitations, the L-39NG is not permitted to land under this crosswind condition; a go-around or diversion to an aerodrome with more favorable wind conditions is required.

Overall, the ANSYS CFX simulations demonstrate that crosswind increases drag, reduces lift, and disrupts the symmetry of the flow field around the L-39NG, with the magnitude of these effects increasing significantly with sideslip angle. The results provide a quantitative basis for assessing the influence of crosswind on the aerodynamic characteristics and landing conditions of the L-39NG.

REFERENCES

1. [Nguyen, H.H., Aerodynamics (For Military Pilots), Air Force Officer’s College, 2023.
2. Lai Cong Hoan, Aerodynamics and Principles of Flight, Air Force Officer’s College, 2010.
3. Technical Description and Operating Manual for the L-39NG Aircraft, Air Force Officer’s College, 2025
4. ANSYS® CFX Solver Theory Guide, ANSYS Inc.
5. Nguyen, V.H., ANSYS and Numerical Simulation in Industry Using the Finite Element Method, Hanoi University of Science and Technology, Hanoi, 2003.
6. David M. P., Georgiy I. S., Aerodynamics, Mashinostroenie Publishing House, Moscow, 1968.
7. Akimov, A.N., Vorobyev, V.V., Demchenko, O.F., et al., Design Features of Light Combat and Trainer Aircraft, edited by N.N. Dolzhenkov and V.A. Podobedov, Mashinostroenie–Polet, Moscow, 2005, 368 p.